Chinese Journal of Natural Medicines

Loganin inhibits the ROS–NLRP3–IL–1 β axis by activating the NRF2/HO–1 pathway against osteoarthritis

Miao LI, Jiacong XIAO, Baihao CHEN, Zhaofeng PAN, Fanchen WANG, Weijian CHEN, Qi HE, Jianliang LI, Shaocong LI, Ting WANG, Gangyu ZHANG, Haibin WANG, Jianfa CHEN

Citation: Miao LI, Jiacong XIAO, Baihao CHEN, Zhaofeng PAN, Fanchen WANG, Weijian CHEN, Qi HE, Jianliang LI, Shaocong LI, Ting WANG, Gangyu ZHANG, Haibin WANG, Jianfa CHEN, Loganin inhibits the ROS–NLRP3–IL–1 β axis by activating the NRF2/HO–1 pathway against osteoarthritis, Chinese Journal of Natural Medicines, 2024, 22(11), 1–14. doi: 10.1016/S1875–5364(24)60555–8.

View online: https://doi.org/10.1016/S1875–5364(24)60555–8

Wechat

Available online at www.sciencedirect.com
ScienceDirect
Chinese Journal of Natural Medicines 2024, **22**(11): 977-990
doi: 10.1016/S1875-5364(24)60555-8
Chinese Journal of Natural Medicines

•Original article•

Loganin inhibits the ROS-NLRP3-IL-1β axis by activating the NRF2/HO-1 pathway against osteoarthritis

LI Miao[1, 2], XIAO Jiacong[1, 2], CHEN Baihao[1, 2], PAN Zhaofeng[1, 2], WANG Fanchen[1, 2], CHEN Weijian[1, 2], HE Qi[1, 2], LI Jianliang[1, 2], LI Shaocong[1, 2], WANG Ting[1, 2], ZHANG Gangyu[1, 3*], WANG Haibin[4*], CHEN Jianfa[4*]

[1] *1st School of Medicine, Guangzhou University of Chinese Medicine, Guangzhou 510405, China;*
[2] *The Laboratory of Orthopaedics and Traumatology of Lingnan Medical Research Center, Guangzhou University of Chinese Medicine, Guangzhou 510405, China;*
[3] *Department of Biomedicine, University of Basel, Basel, Switzerland;*
[4] *Department of Orthopaedics, First Affiliated Hospital, Guangzhou University of Chinese Medicine, Guangzhou 510405, China*

Available online 20 Nov., 2024

[ABSTRACT] Loganin (LOG), a bioactive compound derived from *Cornus officinalis* Siebold & Zucc, has been understudied in the context of osteoarthritis (OA) treatment. In this study, we induced an inflammatory response in chondrocytes using lipopolysaccharide (LPS) and subsequently treated these cells with LOG. We employed fluorescence analysis to quantify reactive oxygen species (ROS) levels and measured the expression of NLRP3 and nuclear factor erythropoietin-2-related factor 2 (NRF2) using real-time quantitative polymerase chain reaction (qRT-PCR), Western blotting, and immunofluorescence (IF) techniques. Additionally, we developed an OA mouse model by performing medial meniscus destabilization (DMM) surgery and monitored disease progression through micro-computed tomography (micro-CT), hematoxylin and eosin (H&E) staining, safranin O and fast green (S&F) staining, and immunohistochemical (IHC) analysis. Our results indicate that LOG significantly reduced LPS-induced ROS levels in chondrocytes, inhibited the activation of the NLRP3 inflammasome, and enhanced NRF2/heme oxygenase 1 (HO-1) signaling. *In vivo*, LOG treatment mitigated cartilage degradation and osteophyte formation triggered by DMM surgery, decreased NLRP3 expression, and increased NRF2 expression. These findings suggest that LOG has a protective effect against OA, potentially delaying disease progression by inhibiting the ROS-NLRP3-IL-1β axis and activating the NRF2/HO-1 pathway.

[KEY WORDS] Loganin; NRF2/HO-1 signaling; ROS-NLRP3-IL-1β axis; Osteoarthritis
[CLC Number] R965 **[Document code]** A **[Article ID]** 2095-6975(2024)11-0977-14

Introduction

Osteoarthritis (OA) is a chronic condition predominantly affecting the elderly, characterized by the degradation of cartilage, the formation of periarticular bone fragments, and subchondral bone sclerosis [1, 2]. Initially, OA typically presents with joint pain, swelling, and deformity, while advanced stages are marked by significant joint dysfunction and restricted mobility [3]. Current treatment strategies primarily focus on managing inflammation and pain through non-steroidal anti-inflammatory drugs (NSAIDs) and glucocorticoids [4]. However, these medications provide only partial relief and can lead to adverse effects with long-term use [5]. In cases of severe OA, surgical interventions remain the only option, imposing substantial burdens on individuals and healthcare-systems [6]. Consequently, there is a critical need for innovative OA treatments that are both effective and carry minimal side effects.

Inflammation is a fundamental pathological factor in the progression of OA [7]. Emerging research highlights the NLRP3 inflammasome as a pivotal contributor to OA exacerbation [8, 9], where its activation promotes Caspase-1 activity, leading to the maturation and release of pro-inflammatory cy-

[Received on] 06-Jan.-2024
[Research funding] This work was supported by the National Natural Science Foundation of China (No. 82074462), the Major Research Project of Guangzhou University of Chinese Medicine (No. 2021xk53), and the First Affiliated Hospital of Guangzhou University of Chinese Medicine National Center for Traditional Chinese Medicine Inheritance and Innovation Special Research (No. 2022QN02).
[*Corresponding author] E-mails: zhang13751880597@163.com (ZHANG Gangyu); hipman@163.com (WANG Haibin); 13760793784@163.com (CHEN Jianfa)
These authors have no conflict of interest to declare.

tokines IL-1β and IL-18, thereby accelerating OA progression [10].

Additionally, oxidative stress is intimately linked with cartilage matrix degradation in OA [11]. An imbalance in reactive oxygen species (ROS) levels within cells triggers changes in chondrocyte signaling, increasing the expression of matrix metalloproteinases (MMPs) and disrupting cartilage metabolism [12]. ROS also plays a role in the formation and activation of the NLRP3 inflammasome [13]. For instance, LIU *et al*. found that reducing ROS levels significantly hindered the NLRP3-mediated secretion of inflammatory cytokines [14]. Recent studies also suggest the involvement of the ROS-NLRP3-IL-1β axis in the inflammatory activation observed in conditions such as dry eye and myeloproliferative diseases [15, 16]. Investigating the dynamics of this axis in chondrocytes may thus offer new directions for addressing arthritis more effectively.

Nuclear factor erythropoietin-2-related factor 2 (NRF2) is a crucial oxidative regulator *in vivo*, implicated in various diseases [17]. ZENG *et al*. observed that activation of NRF2 signaling curtailed ROS production and NLRP3 inflammasome activity [18]. Conversely, inhibiting NRF2 signaling heightened ROS-mediated activation of these inflammasomes [19]. Heme oxygenase 1 (HO-1) is known for its significant anti-inflammatory, antioxidant, and anti-apoptotic properties [20]. Consequently, the NRF2/HO-1 signaling pathway, with its comprehensive protective capabilities against inflammation, oxidative stress, and cell death, is vital for the oxidative stress response, offering protection across multiple organs and aiding in the treatment of specific diseases [21, 22]. Although direct evidence linking NRF2/HO-1 with cartilage protection is scant, extensive research indicates that activating this pathway can shield cartilage from oxidative damage [23, 24]. Additionally, enhancing NRF2's nuclear translocation to modulate the NF-κB pathway has been well documented to produce anti-inflammatory effects in OA [25, 26].

Loganin (LOG), the primary active constituent of the traditional Chinese medicinal herb *Cornus officinalis* Siebold & Zucc, has been utilized in treating OA [27, 28]. It is recognized for its anti-inflammatory, antioxidant, and anti-diabetic effects [29]. Previous studies have demonstrated that LOG can mitigate acute kidney injury by modulating the NRF2/HO-1 signaling [30], and recent findings suggest that it reduces ROS production and NLRP3 inflammasome activation in high glucose-induced Schwann cells [31]. Moreover, HU *et al*. revealed that LOG alleviates OA by inhibiting NF-κB signaling [27]. However, the specific effects of LOG on ROS reduction and NLRP3 inflammasome activation in chondrocytes remain to be elucidated.

This study aimed to explore whether LOG can inhibit the ROS-NLRP3-IL-1β axis by activating the NRF2/HO-1 pathway, thereby exerting anti-inflammatory and antioxidant effects conducive to treating OA.

Materials and Methods

Reagents

LOG (CAS No. 18524-94-2) was obtained from RuiFenSi Company (Chengdu, China). Lipopolysaccharide (LPS) and collagenase type II were purchased from Sigma (Stuttgart, Germany). Primer (Table 1) was obtained from Tsingke Biotechnology (Beijing, China). ML385 (Nrf2 specific inhibitor) was purchased from MedChemExpress (NJ, USA). Primary antibodies against *β*-actin (Cat. No. AF7018), NRF2 (Cat. No. AF0639), matrix metallopeptidase 3 (MMP3, Cat. No. AF0217), type II collagen (Col2, Cat. No. AF0135), HO-1 (Cat. No. AF5393) and the secondary antibody (Cat. No. DF6681) were obtained from Affinity Biosciences (Jiangsu,China),andCaspase-1/Cleavedcaspase-1(Cat.No.WL03-450), IL-1β (Cat. No. WL00891), pro-interleukin-1β (pro-IL-1β, Cat. No. WL02257), NLRP3 (Cat. No. WL02635), and IL-18 (Cat. No. WL01127) were obtained from Wanleibio (Shenyang, China).

Cell culture

Chondrocytes were isolated from the knee cartilage of 7-day-old C57BL/6J mice, which were euthanized under deep anesthesia. The cartilage was excised, finely minced, and then subjected to enzymatic digestion. This involved 30-min incubation in 0.25% trypsin, followed by 7-h digestion in 0.25% type II collagenase, until the chondrocytes were successfully isolated [32]. The harvested chondrocytes were cultured in DMEM/F12 medium supplemented with 10% fetal bovine serum (FBS) and maintained at 37 °C in a humidified incubator with 5% CO_2. Chondrocytes from the second to fifth passages were used for the experiments.

Cell viability assay

For the viability assays, chondrocytes were seeded in 96-

Table 1 Quantitative real-time PCR primer sequences

Genes	Forward (5′-3′)	Reverse (5′-3′)
18s rRNA	TGGTTGCAAAGCTGAAACTTAAAG	AGTCAAATTAAGCCGCAGGC
Col2	CTCCTTCCAGGTCCCA	CTTCCGTCAGCGTCAACACC
Mmp3	TGCTTCCCAATCCTATTTGC	AGAATCCCTTTCCCTCTCCA
Nlrp3	ATTACCCGCCCGAGAAAGG	TCGCAGCAAAGATCCACACAG
Caspase-1	AACAGAACAAAGAAGATGGCACA	CCAACCCTCGGAGAAAGAT
Il-1β	GAAATGCCACCTTTTGACAGTG	TGGATGCTCTCATCAGGACAG
Il-18	TGGAGACCTGGAATCAGACA	TGGGGTTCACTGGCACTT

well plates at a density of 1×10^3 cells per well. Cells were treated with varying concentrations of LOG (1, 2.5, 5, 10, 25, 50, 100 μmol·L^{-1}) in the presence or absence of LPS (1 μg·mL^{-1}) for either 24 or 48 h [33]. Following treatment, 10 μL of CCK-8 solution was added to each well, and the cells were incubated for an additional 2 h. The absorbance was then measured at 450 nm to assess cell viability.

Toluidine blue staining

For histological analysis, chondrocytes were plated at a density of 3×10^4 cells per well in 24-well plates and treated with LOG (5, 10 μmol·L^{-1}) with or without LPS (1 μg·mL^{-1}) for 48 h. Post-treatment, cells were washed with PBS, fixed in 4% paraformaldehyde for 20 min at room temperature, and washed again. Cells were then stained with 1% toluidine blue for 1 h at room temperature, rinsed thrice with PBS, and examined under a light microscope.

Quantitative real-time PCR (qRT-PCR)

Chondrocytes were treated with LOG at concentrations of 5 and 10 μmol·L^{-1}, with or without LPS (1 μg·mL^{-1}) for 48 h. Total RNA was subsequently extracted using Trizol reagent (AG, China). For cDNA synthesis, an Evo M-MLV RT Kit (AG, China) was utilized. mRNA levels were quantified using the Bio-Rad CFX96 Real-Time System and SYBR Green Pro Taq (AG, China), according to the manufacturer's protocol.

Western blotting analysis

Total proteins were extracted from chondrocytes using RIPA buffer (Beyotime, China). Concentrations were determined using a BCA assay kit (Biosharp, China). The proteins were separated by electrophoresis on a 4%−15% Sodium Dodecyl Sulfate PolyAcrylamide Gel Electrophoresis (SDS-PAGE) gel and transferred to polyvinylidene fluoride (PVDF) membranes. These membranes were blocked with 5% bovine serum albumin (BSA) solution for 1.5 h, incubated overnight at 4 °C with primary antibodies, and then for 1.5 h with secondary antibodies at room temperature. Detection was performed using an Electrochemiluminescence (ECL) system, and images were captured for analysis.

Determination of ROS levels

Following treatment with LOG and LPS, chondrocytes were incubated in a serum-free medium with dihydroethidium (DHE, Beyotime, China) at 37 °C for 20 min in a light-protected environment. After two Phosphate-buffered saline (PBS) washes, cells were stained with Hoechst 33342 (Beyotime, China) for 8 min, followed by another two washes. Intracellular ROS fluorescence was then observed under a Leica microscope. Additionally, cells were digested, centrifuged, and re-incubated with dichlorofluorescein diacetate (DCFH-DA, Beyotime, China) at 37 °C for 20 min, shielded from light. After washing and resuspension in PBS, intracellular ROS levels were quantified using flow cytometry (BD Biosciences, USA)

Determination of malondialdehyde (MDA) and super oxide dismutase (SOD)

Chondrocytes were exposed to LOG of 5 and 10 μmol·L^{-1}, with or without LPS (1 μg·mL^{-1}) for 48 h. Subsequently, MDA and SOD levels were measured using assay kits according to the manufacturer's instructions provided by Beyotime, China.

Immunofluorescence (IF)

Cells were first fixed with 4% polymethanol for 15 min at room temperature and then permeabilized with 0.2% Triton X-100 for 30 min. After blocking with 4% BSA for 1 h at room temperature, the cells were incubated with primary antibodies against NRF2, NLRP3, and Col2 at a 1 ∶ 200 dilution overnight at 4 °C. Following this, cells were incubated with a red fluorescence-labeled secondary antibody at a 1 ∶ 250 dilution for 1 h at room temperature. Nuclei were stained with DAPI for 3 min, and the cells were examined using confocal laser scanning microscopy to capture IF images.

Molecular docking

The structural formula of LOG was obtained from the PubChem website (https://pubchem.ncbi.nlm.nih.gov/), and its 3D structure was created using Chem3D software and exported in mol*2 format. The structural domain of the core protein NRF2 was downloaded in PDB format from the Protein Data Bank (http://www.rcsb.org/), prepared by removing water and phosphate groups using PyMOL software (version 2.3, DeLano Scientific LLC). Both the LOG and NRF2 structures were converted to pdbqt format using AutoDockTools (version 1.5.6). The Vina script was employed to identify the active pockets and calculate the molecular binding energies. The interactions, including the LibDockScore of flexible binding, were analyzed using Discovery Studio (version 2019, DNASTAR). Molecular docking results were then visualized in two-dimensional and three-dimensional formats using PyMOL software to illustrate the potential binding conformations and interactions between LOG and NRF2.

Animal experiment

Seven-week-old male C57BL/6J mice were sourced from the Guangzhou University of Chinese Medicine. The experimental protocol was approved by the Ethics Committee of the First Affiliated Hospital of Guangzhou University of Chinese Medicine, complying with the National Institutes of Health ethical guidelines (approval number: GZTCMF1-2022117; January 17, 2022). Mice, except for those in the control group, underwent destabilization of the medial meniscus (DMM) surgery to establish an OA model [34]. Post-surgery, mice were categorized into four groups: control (n = 8), model (n = 8), LOG-L (low dose LOG, 50 mg·kg^{-1}, n = 8), LOG-H group (high dose LOG, 100 mg·kg^{-1}, n = 8), based on the dosages determined from previous studies [35]. Both the control and model groups were administered equivalent volumes of saline by gavage. After eight weeks of treatment, the mice were euthanized to harvest their lower limbs for subsequent analysis.

Micro-computed tomography (micro-CT) scanning

The harvested lower limbs were fixed in 4% paraformaldehyde for 24 h and subsequently stored in PBS. Micro-CT

scanning of the knee joints was performed, followed by 3D reconstruction and detailed joint analysis. Assessment of subchondral bone involved measuring metrics such as bone volume fraction (BV/TV), trabecular separation (Tb.Sp), trabecular thickness (Tb.Th), and trabecular number (Tb.N).

Histological analysis

Post-fixation, the samples underwent a two-week decalcification process using 14% ethylenediaminetetraacetic acid (EDTA). They were then embedded in paraffin and sectioned into 5-micron slices. These sections were placed on slides, baked to ensure adhesion, and then subjected to a graded series of xylene and ethanol for rehydration, each step lasting 3 min. After rinsing with distilled water and PBS, the sections were stained with hematoxylin and eosin (H&E) and safranin O and fast green (S&F), adjusting staining times according to preliminary microstaining results. Following staining, sections were dehydrated in ascending concentrations of ethanol and xylene, each for 3 min, then air-dried, and mounted with a drop of neutral gum. The stained sections were imaged under a microscope to evaluate morphological and pathological changes.

Immunohistochemistry

For immunohistochemical analysis, knee tissue sections were first deparaffinized using xylene and rehydrated through a series of anhydrous ethanol solutions. Antigen retrieval was performed using a sodium citrate solution. Sections were then blocked with sheep serum for 10 min at room temperature to prevent non-specific binding. Subsequently, sections were incubated overnight at 4 °C with primary antibodies against NRF2 and NLRP3, both diluted at 1 ∶ 200. After primary antibody incubation, sections were exposed to secondary antibodies for 30 min at room temperature. Staining was conducted using a DAB solution, followed by counterstaining with hematoxylin to enhance nuclear visibility. The sections were then sealed with resin, and images were captured under a microscope for analysis.

Statistical analyses

Statistical analyses were performed using SPSS version 25.0. Data were expressed as mean ± standard deviation (SD). For normally distributed data with homogeneous variance, one-way analysis of variance (ANOVA) was used for comparisons among multiple groups, while the *t*-test was applied for pairwise comparisons. For data with non-homogeneous variance, Dunnett's T3 test was utilized. A *P*-value of less than 0.05 was deemed to indicate statistical significance. All experiments were replicated at least three times to ensure consistency and reliability of the results.

Results

Effects of LOG on cell viability in LPS-treated chondrocytes

In this study, we induced inflammation in chondrocytes using LPS (1 μg·mL^{-1}) to establish an inflammatory model [33]. Chondrocytes are identified in Fig. S1. As shown in Figs. 1B and 1C, LPS exposure was found to inhibit chondrocyte proliferation; however, treatment with LOG enhanced cell viability in a dose-dependent manner. Notably, a concentration of 10 μmol·L^{-1} LOG displayed the most significant protective effect on chondrocytes. Higher concentrations, such as 25 μmol·L^{-1}, showed inhibitory effects on chondrocyte proliferation, leading to the selection of 5 and 10 μmol·L^{-1} for further experiments. Additionally, LPS treatment resulted in chon-

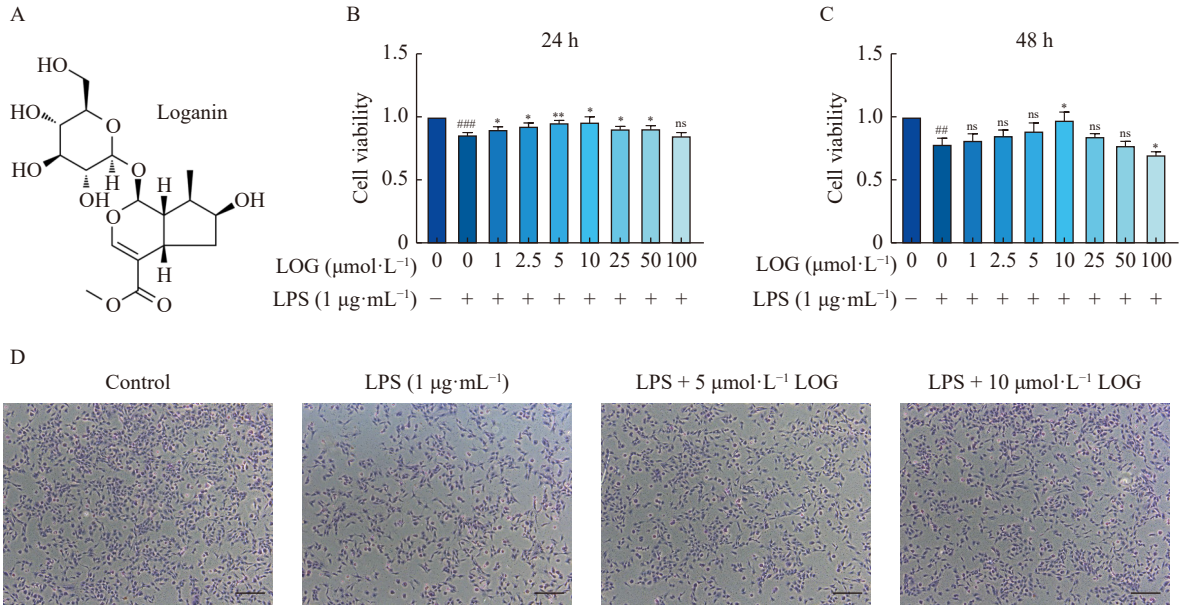

Fig. 1 LOG attenuates the inhibition of proliferation induced by LPS in chondrocytes. (A) Chemical Structure of LOG. (B, C) Effect of different concentrations of LOG (1, 2.5, 5, 10, 25, 50, 100 μmol·L^{-1}) on cell viability in the presence or absence of LPS for 24 or 48 h. (D) Toluidine blue staining of chondrocytes morphology (Scale bar: 100 μm). Data are presented as the mean ± SD (n = 3). $^{*}P$ < 0.05, $^{**}P$ < 0.01, $^{***}P$ < 0.001 *vs* the control group; $^{\#\#}P$ < 0.01, $^{\#\#\#}P$ < 0.001 *vs* the LPS treated group (ns: not significant).

drocytes that were enlarged and had increased tentacles, a phenomenon that was mitigated by LOG treatment (Fig. 1D).

LOG alleviates ECM degradation in chondrocytes

Collagen type II (Col2) is a primary component of the extracellular matrix (ECM), while matrix metalloproteinase-3 (MMP3) serves as an enzyme [36] that degrades the ECM. To assess the protective effects of LOG on chondrocyte homeostasis, we analyzed the expression levels of Col2 and MMP3 *via* qRT-PCR and Western blotting assays. The results revealed that LPS exposure decreased Col2 expression and increased MMP3 levels at both mRNA (Figs. 2A−2C) and protein levels (Figs. 2D and 2E). Treatment with LOG, particularly at concentrations of 5 and 10 μmol·L^{-1}, partially reversed these adverse effects. IF studies further confirmed these findings, showing that LOG treatment restored Col2 fluorescence intensity close to control levels, especially in the high-concentration group (Fig. 2F).

LOG reduces LPS-induced ROS production

ROS is critical in maintaining metabolic homeostasis in chondrocytes [37]. However, excessive ROS production can lead to oxidative stress and accelerate OA progression [12]. Our study utilized ROS probe staining by fluorescence microscopy (Fig. 3A) and flow cytometry (Fig. 3B) to evaluate ROS levels. The results demonstrated that LPS significantly increased ROS production, whereas LOG-treated cells exhibited reduced ROS fluorescence intensity, suggesting a decrease in ROS production (Figs. 3A−3D). To further quantify the oxidative stress, we measured intracellular levels of malondialdehyde (MDA) and superoxide dismutase (SOD) activity. LPS treatment markedly raised MDA levels and reduced SOD activity, while LOG treatment effectively decreased MDA levels and enhanced SOD activity (Figs. 3E

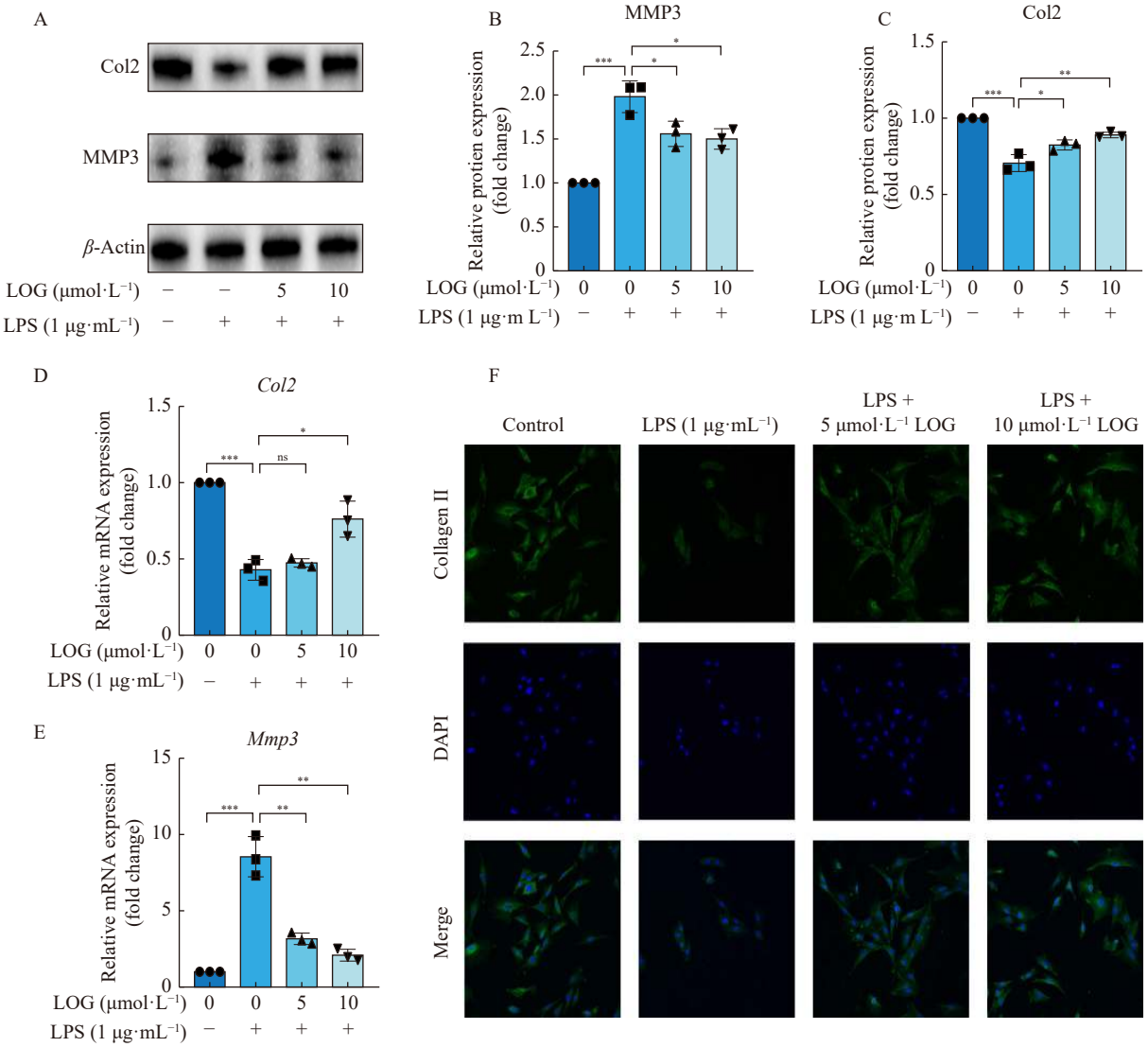

Fig. 2 LOG alleviates ECM degradation in chondrocytes. (A) Representative images and (B, C) quantitative analysis of Western blots of Col2 and MMP3. All experiments were repeated three times. (D, E) Gene expressions of *Col2* and *Mmp3* detected by qRT-PCR. (F) IFof Col2 (green) and DAPI-stained nuclear fluorescence (blue) were visualized by confocal microscopy (Scale bar: 10 μm). Data are presented as the mean ± SD (n = 3). $^{*}P < 0.05$, $^{**}P < 0.01$, $^{***}P < 0.001$ (ns: not significant).

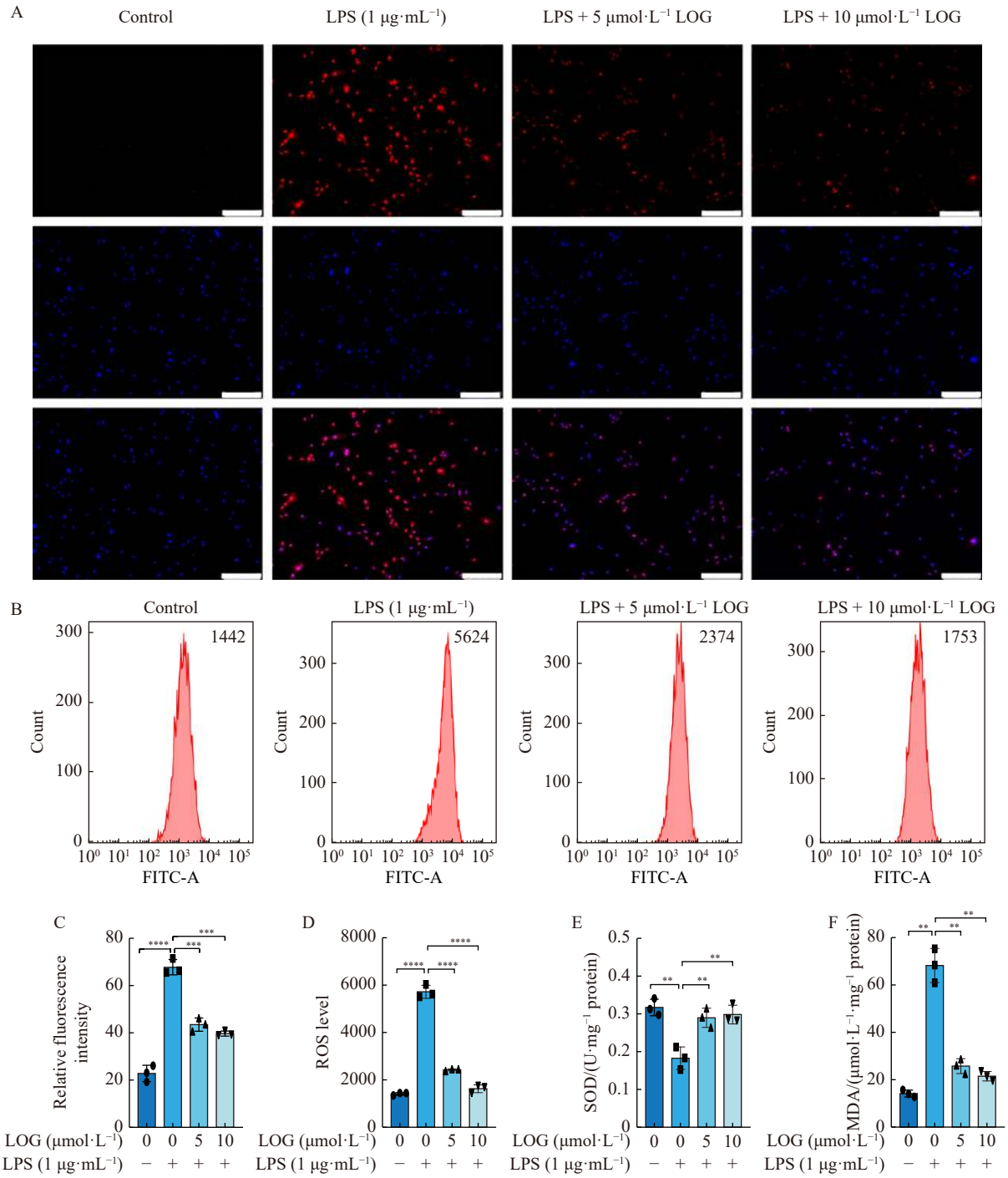

Fig. 3 LOG reduces LPS-induced ROS production. (A) Representative images of immunofluorescent staining and (B) flow cytometric analysis of ROS levels in chondrocytes treated with LPS or LOG (magnification: 10 ×; Scale bar: 100 μm). (C) Relative fluorescence intensity of (A). (D) Quantitative histogram of ROS levels. (E) SOD activity and (F) MDA levels in chondrocytes. Data are presented as the mean ± SD (n = 3). $^{*}P < 0.05$, $^{**}P < 0.01$, $^{***}P < 0.001$, $^{****}P < 0.0001$ (ns: not significant).

and 3F), indicating that LOG can mitigate LPS-induced oxidative stress in chondrocytes. However, LOG significantly reduced MDA levels and increased SOD activity (Figs. 3E and 3F). Our results showed that LOG is capable of resisting LPS-induced oxidative stress damage in chondrocytes.

LOG suppresses NLRP3 inflammasome activation

Emerging evidence underscores the critical role of the NLRP3 inflammasome in the progression of OA. This complex is activated by increased ROS production, leading to caspase-1 activation, which then stimulates the release of pro-inflammatory cytokines IL-1β and IL-18, exacerbating inflammation [38]. Our findings indicated that LPS treatment significantly upregulated the expression of IL-1β, NLRP3, cleaved caspase-1, and IL-18 in chondrocytes at both the

mRNA and protein levels (Figs. 4A−4I). Conversely, LOG treatment effectively reduced the expression of these inflammatory mediators. IF analysis further revealed that NLRP3 expression was markedly elevated in the chondrocytes of the

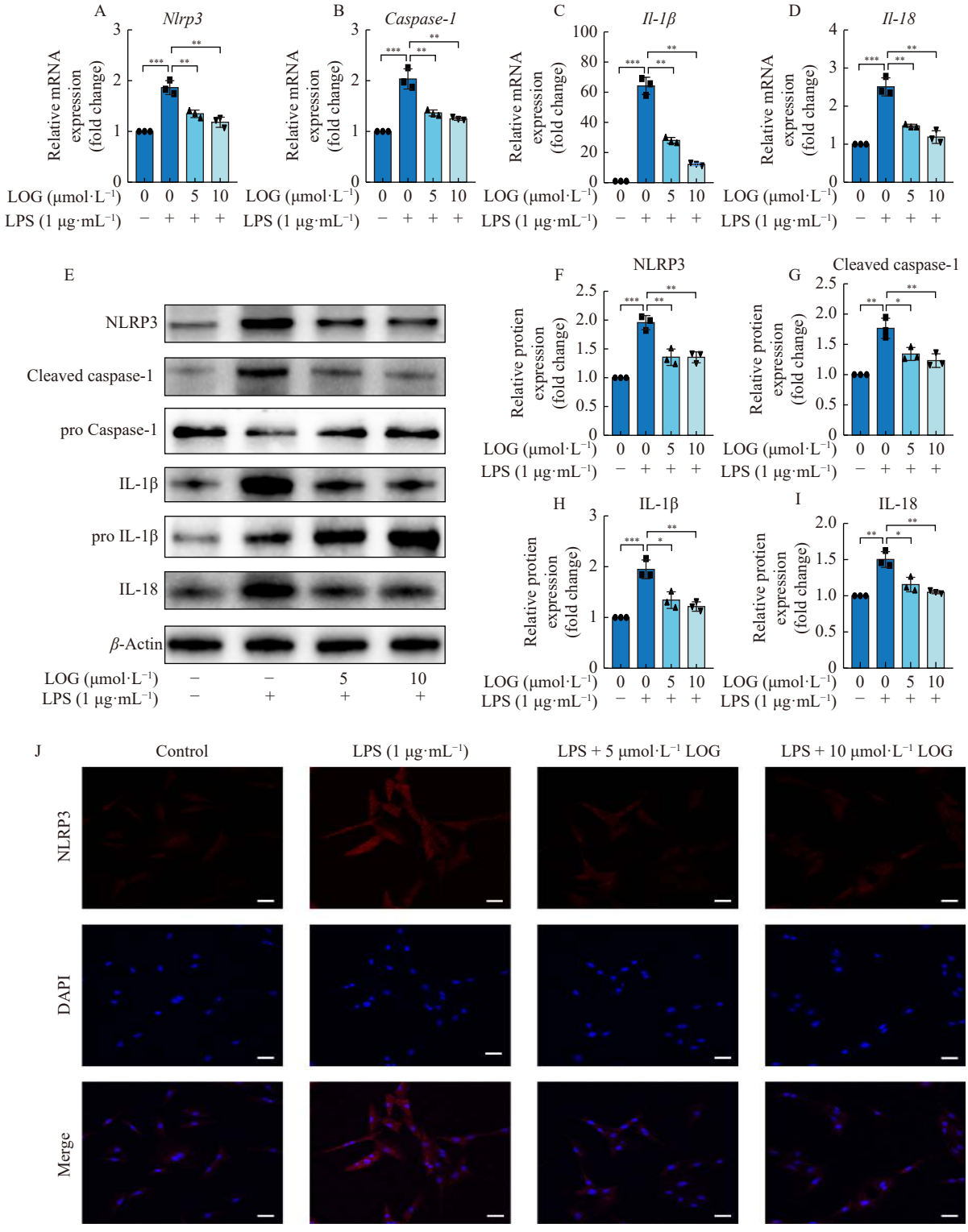

Fig. 4 LOG suppresses NLRP3 inflammasome activation. (A−D) Gene expressions of *Nlrp3*, *Caspase-1*, *IL-1β*, and *IL-18* detected by qRT-PCR. (E) Representative images and (F−I) quantification of Western blots of NLRP3, Cleaved caspase-1, pro-Caspase-1, IL-1β, pro-IL-1β, and IL-18. All experiments were repeated three times. (J) IF of NLRP3 (red) and DAPI-stained nuclear fluorescence (blue) were visualized by confocal microscopy (Scale bar, 10 μm). Data are presented as the mean ± SD (n = 3). $^{*}P$ < 0.05, $^{**}P$ < 0.01, $^{***}P$ < 0.001 (ns: not significant).

model group, whereas LOG treatment, particularly at higher doses, significantly decreased NLRP3 expression (Fig. 4J). These observations were corroborated by *in vivo* immunohistochemistry results.

LOG activates the NRF2/HO-1 signaling

ROS is implicated in triggering the activation of the NLRP3 inflammasome. NRF2 is a direct downstream pathway of ROS, which regulates cellular redox homeostasis [39]. To investigate whether LOG inhibits ROS-mediated NLRP3 inflammasome activation *via* the NRF2/HO-1 pathway, we employed network pharmacology and molecular docking assays to examine the interaction between LOG and NRF2. The docking studies showed favorable binding energies below −5.0 kcal·mol^{-1} and RMSD values, and the LibDockScores of the docking models formed were all greater than 100 (If the binding energy is less than 0, the ligand and receptor can spontaneously bind, and if the Vina binding energy is ≤ −5.0 kcal·mol^{-1} and LibDock can find the docking site and LibDockScore > 100, the two are stably docked). Combined with the RMSDs, chemical energies, and docking scores, the binding energies of the active ingredient LOG and the core protein NRF2 could form stable docking. We utilized the compound results exported from Vina to import into Pymol and then demonstrated 3-dimensional and 2-dimensional molecular docking with protein ligands using Discovery Studio 2019 software (Figs. 5A−5C). Next, we found that LPS slightly increased the expression of NRF2 and HO-1 compared with the control group (Figs. 5D−5F). However, both 5 and 10 μmol·L^{-1} LOG treatment significantly increased the expression of NRF2 and HO-1 (Figs. 5D−5F). In response to oxidative stress, NRF2 undergoes ubiquitination, accumulates intracellularly, and translocates to the nucleus, promoting its antioxidant transcriptional program [40]. The results in Fig. 5G show that the expression of NRF2 in the control group was concentrated in the cytoplasm, while under LPS stimulation, NRF2 clustered toward the nucleus but could not enter the nucleus, and after drug treatment, the expression of NRF2 was concentrated in the nucleus, suggesting that LOG could promote its entry into the nucleus and thus exert antioxidant function (Figs. 5G and 5H). IHC staining of the mouse articular cartilage showed that the expression of NRF2 was significantly higher in the LOG group, which is consistent with the *in vitro* results (Figs. 8D and 8H).

To further substantiate the role of LOG in activating NRF2 signaling, we utilized the NRF2-specific inhibitor ML385. The results demonstrated that ML385 negated the ROS-reducing effect of LOG (Figs. 6A and 6B). Additionally, Western blot analyses revealed that ML385 also obstructed the suppressive impact of LOG on inflammatory mediators such as IL-1β, NLRP3, Cleaved caspase-1, and IL-18 and inhibited the activation of the NRF2/HO-1 signaling pathway (Figs. 6C−6J). These findings support the hypothesis that LOG mitigates ROS production and subsequent inflammation primarily through the activation of NRF2/HO-1 signaling, thereby effectively inhibiting NLRP3 inflammasome activation. This mechanism is crucial for the anti-inflammatory effects of LOG in the context of OA.

LOG alleviates DMM-induced OA in mice

Inflammation, cartilage degeneration, and periarticular bone reconstruction are hallmark characteristics of OA [2]. Our study employed a destabilization of the DMM surgery to induce OA in mice and assessed the therapeutic effects of LOG on this model. The micro-CT scans showed that LOG treatment led to a notable reduction in periarticular bone formation compared to the DMM group (Figs. 7A and 7B). Quantitative analysis of subchondral bone histology revealed improvements with LOG treatment: increased Tb.Th and BV/TV, along with a decrease in Tb.Sp. However, the Tb.N did not show significant differences across the groups (Figs. 7C−7F). These findings suggest that LOG, particularly at higher doses, effectively promotes subchondral bone reconstruction. H&E staining of synovial tissues indicated that LOG mitigated synovial inflammation in the OA mice. This was evident from reduced inflammatory cell infiltration, diminished vascular proliferation, and lower synovitis scores compared to the model group (Fig. 8A). This was reflected in less inflammatory cell infiltration, vascular proliferation, and synovitis scores (Fig. 8E). S&F staining of the articular cartilage further demonstrated that LOG treatment resulted in smoother, thicker, and less worn cartilage surfaces compared to those in the DMM group (Fig. 8B). The therapeutic efficacy of LOG was also quantified using the Osteoarthritis Research Society International (OARSI) scoring system. Our results showed that LOG significantly reduced the OARSI scores in the OA mice, indicating a reduction in OA severity (Fig. 8F). Collectively, these results suggested that LOG can effectively alleviate the progression of DMM-induced OA in mice.

Discussion

ROS-mediated oxidative stress and subsequent activation of the NLRP3 inflammasome play critical roles in the pathogenesis of OA [11]. Under normal conditions, ROS are present at low levels in chondrocytes, primarily participating in intracellular signaling [41]. However, in OA, chondrocytes produce large amounts of ROS, primarily through NADPH oxidase activated under mechanical stimulation and inflammatory conditions [42]. Excessive ROS production exacerbates cartilage degradation by inhibiting matrix synthesis, impeding chondrocyte migration and growth factor activity, and directly breaking down matrix components *via* activation of MMPs. It also leads to chondrocyte apoptosis [43]. Additionally, the overaccumulation of ROS diminishes the activity of SOD, boosts the production of lipid peroxides such as MDA, and weakens the overall antioxidant capacity of chondrocytes [44]. Prior studies have shown that reducing ROS levels can mitigate cartilage degradation in OA [45].

Moreover, ROS has been identified as a pivotal molecule in the activation of the NLRP3 inflammasome [46]. Normally, the thioredoxin interacting protein (TXNIP) is bound

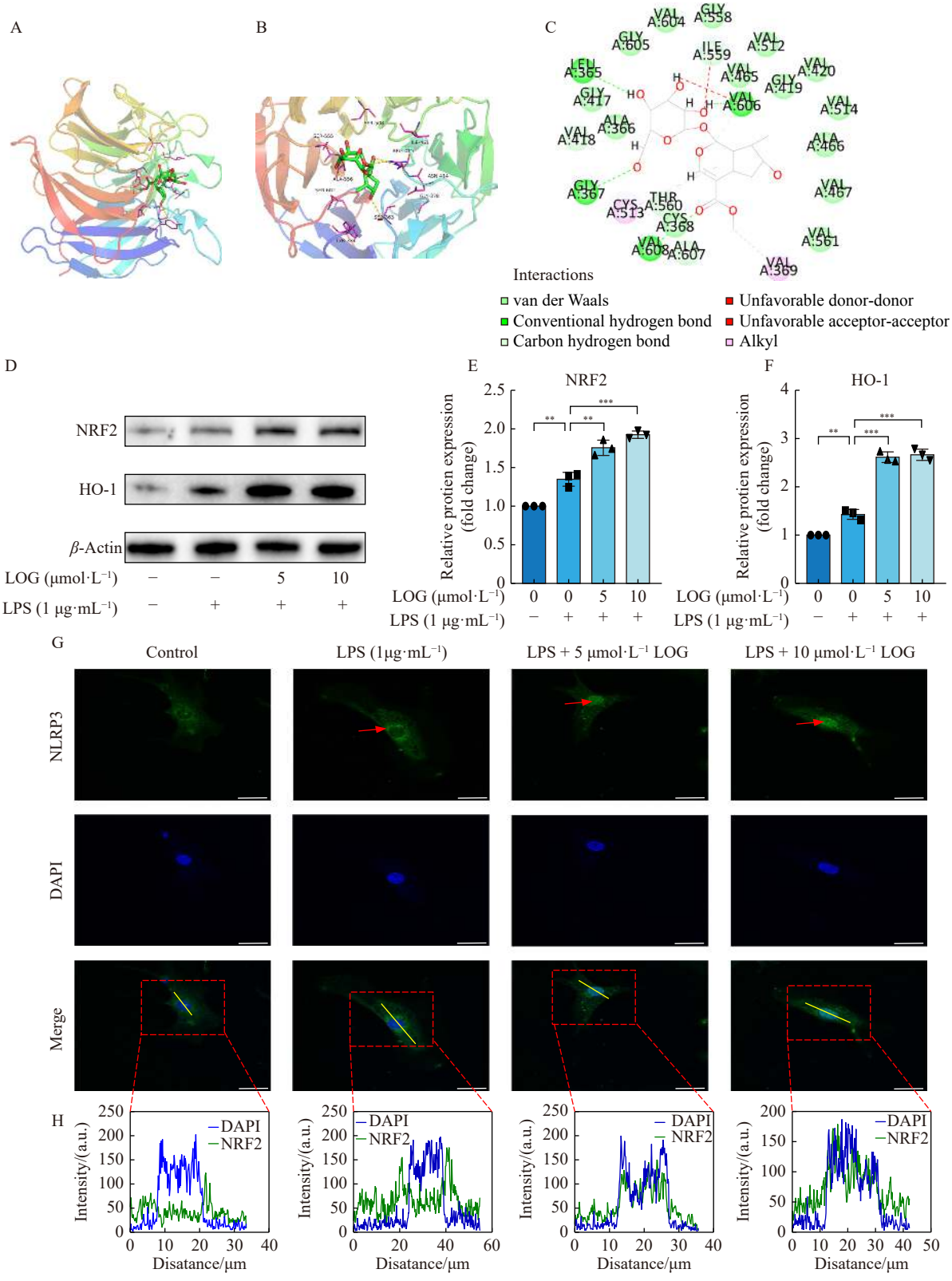

Fig. 5 LOG activates the NRF2/HO-1 signaling pathway. (A) 3D macroscopic docking diagram of NRF2 with LOG. (B) 3D microscopic docking diagram of NRF2 and LOG. (C) 2D docking diagram of NRF2 and LOG. (D) Representative images and (E, F) quantitative analysis of the Western blots of NRF2 and HO-1. All experiments were repeated three times. (G) IF of NRF2 (green) and DAPI-stained nuclear fluorescence (blue) were visualized by confocal microscopy (Scale bar, 25 μm). (H) Co-localization analysis of NRF2 into nuclei in (G) was performed using Image J software. Data are presented as the mean ± SD (n = 3). $^{**}P$ < 0.01, $^{***}P$ < 0.001 (ns: not significant).

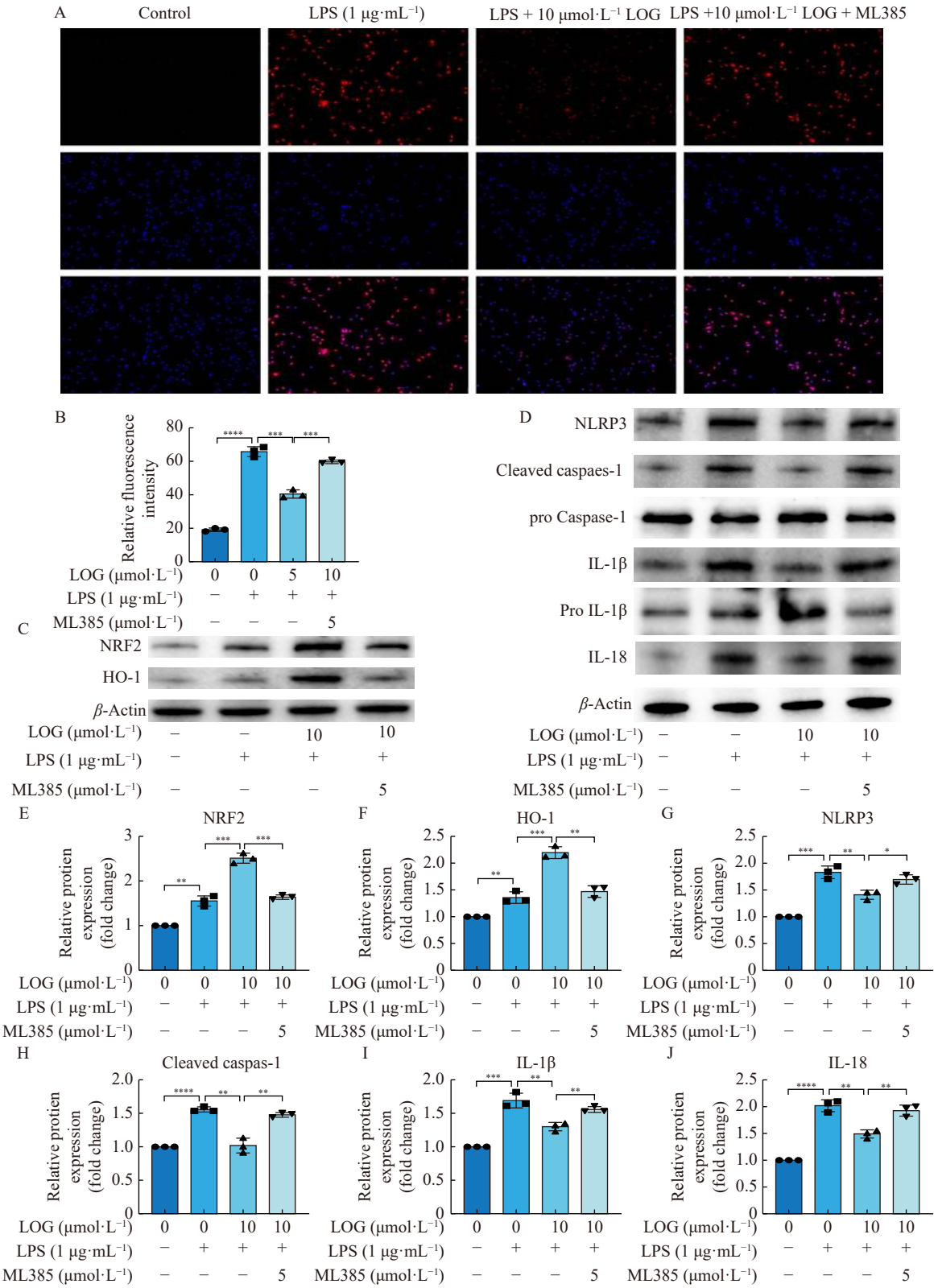

Fig. 6 LOG alleviates ROS-mediated NLRP3 inflammasome activation *via* NRF2/HO-1 signaling. (A) Representative images of DHE staining under a fluorescent microscope (magnification: 10 ×; scale bar: 100 μm). (B) Relative fluorescence intensity of (A). (C, D) Representative images and (E−J) quantitative analysis of Western bolt of NRF2, HO-1, NLRP3, Cleaved caspase-1, Pro Caspase1, IL-1β, Pro IL-1β and IL-18. Data are presented as the mean ± SD (n = 3). $^{*}P < 0.05$, $^{**}P < 0.01$, $^{***}P < 0.001$, $^{****}P < 0.0001$ (ns: not significant).

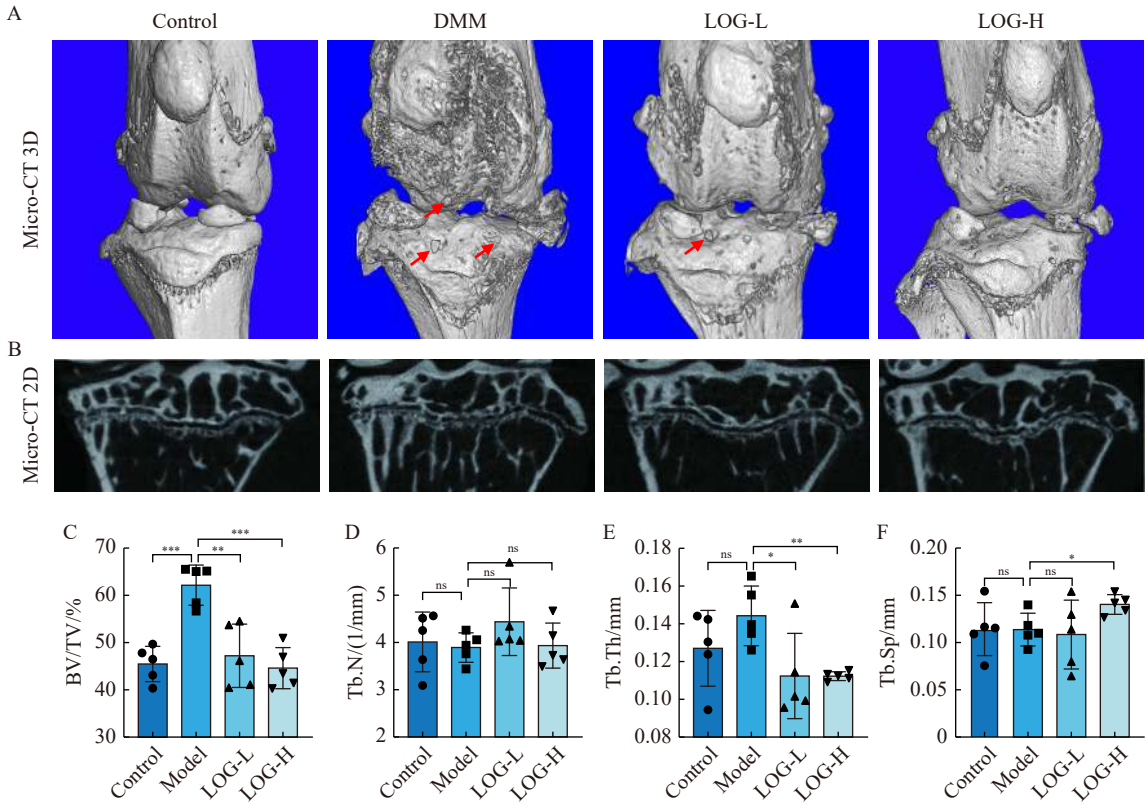

Fig. 7 LOG improves subchondral bone reconstruction. (A) Representative Micro-CT 3D images of the mouse knee joint. Red arrows indicate osteophytes. (B) Representative Micro-CT 2D images of mice subchondral bone. (C−F) Quantitative analysis of BV/TV, Tb.Th, Tb.N, Tb.Sp of subchondral bone. Data are presented as the mean ± SD (n = 8). $^{*}P < 0.05$, $^{**}P < 0.01$, $^{***}P < 0.001$ (ns: not significant).

to thioredoxin (TRX) in a quiescent state [47]. Elevated ROS levels disrupt this TXNIP-TRX complex, leading TXNIP to bind to the leucine-rich repeat (LRR) domain of NLRP3, triggering its oligomerization and activating the inflammasome, thereby promoting an inflammatory response [48, 49]. Studies by Bauernfeind *et al*. revealed that ROS inhibitors can block the priming of the NLRP3 inflammasome [50]. LIN *et al*. indicated that the elimination of ROS in murine OA reduced LPS-induced NLRP3 inflammasome activation [51]. These studies suggested that targeting ROS-mediated NLRP3 in-

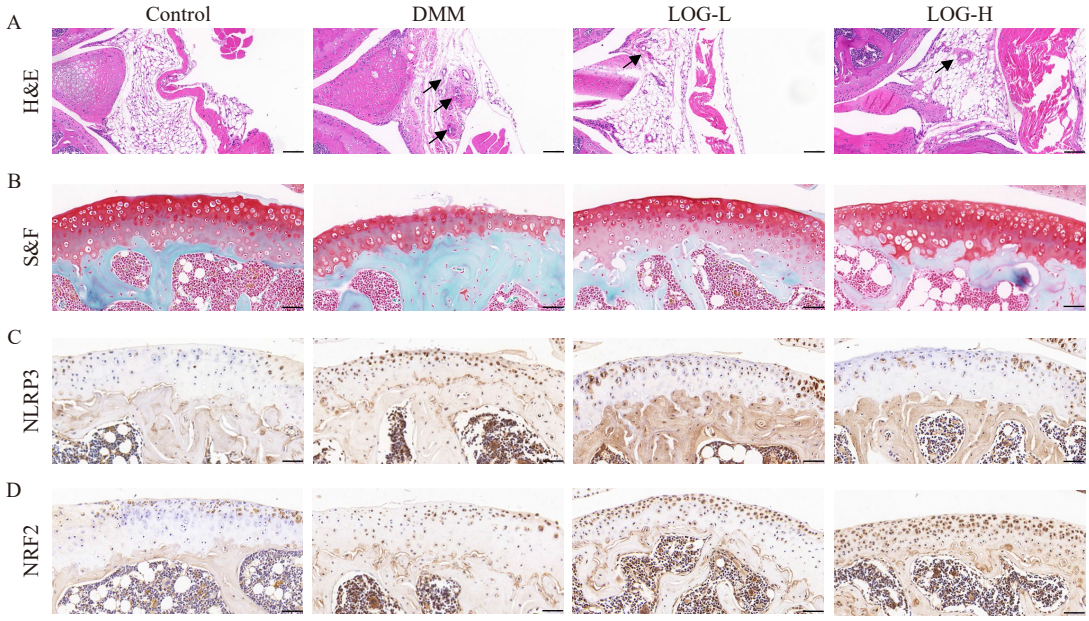

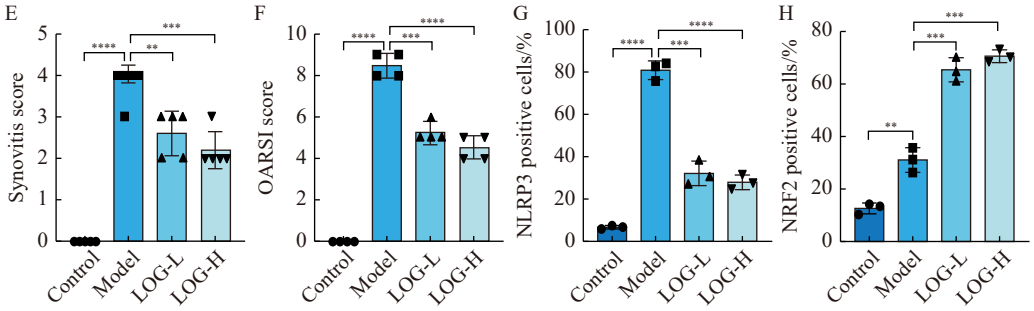

Fig. 8 LOG alleviates DMM-induced OA in mice. (A) Representative images of H&E staining of mice knee joint after eight weeks of LOG treatment. Black arrows indicate inflammatory cell infiltration and blood vessel invasion (magnification: 20 ×; scale bar: 50 μm). (B) Representative images of S&F staining of the articular cartilage (magnification: 20 ×; scale bar: 20 μm). (D, E) Immunohistochemistry staining of NLRP3 and NRF2 and quantitative analysis (G, H) (magnification: 20 ×; scale bar: 20 μm). (E, F) OASI score and synovitis score. Data are presented as the mean ± SD (n = 8). $^{**}P < 0.01$, $^{***}P < 0.001$, $^{****}P < 0.0001$ (ns: not significant).

flammasome activation may be a viable therapeutic strategy for OA. In our study, LPS treatment was used to simulate an inflammatory environment in chondrocytes, resulting in increased expression of MMP3 and decreased expression of Col2, indicative of disrupted chondrocyte homeostasis. Additionally, this inflammatory stimulus led to reduced SOD and glutathione (GSH) levels and increased MDA levels, further evidencing oxidative stress. Treatment with LOG was found to ameliorate these adverse effects. Specifically, LOG treatment significantly reduced the production of ROS induced by LPS, thereby alleviating the oxidative stress and associated cellular damage. This suggests that LOG has potent anti-inflammatory and antioxidant effects that contribute to its therapeutic potential in the treatment of OA, highlighting its ability to restore chondrocyte homeostasis and suppress inflammatory pathways.

The NLRP3 inflammasome complex, comprising NLRP3, ASC, and Caspase-1, plays a pivotal role in the inflammatory response [52]. Exposure to stimuli such as ROS activates NLRP3, which in turn triggers Caspase-1 activation [53]. This activation cascade mediates the maturation of IL-18 and IL-1β, significantly increasing the release of inflammatory factors and promoting cellular inflammation and death [54]. Previous studies highlight the involvement of the NLRP3 inflammasome in OA progression [8]. LI *et al*. demonstrated that NLRP3 activation is linked to reductions in chondrocyte pyroptosis and extracellular matrixdegradation [55], while NI *et al*. found that the NLRP3 inhibitor MCC950 decreased NLRP3 expression in OA cartilage, thereby delaying cartilage degeneration [56]. In our study, LPS stimulation increased ROS levels in chondrocytes, which was associated with upregulated expression of NLRP3, Caspase-1, IL-18, and IL-1β. Treatment with LOG effectively downregulated these expressions and restored the expression levels of proteins related to extracellular matrix degradation. These findings suggest that the ROS-NLRP3-IL-1β axis may contribute to OA progression by promoting inflammation and matrix degradation, while LOG can mitigate OA progression by inhibiting this axis.

The NRF2/HO-1 signaling pathway functions as an endogenous antioxidant system activated during oxidative stress [22]. Elevated ROS levels stimulate NRF2, enhancing the transcription of antioxidant proteins such as HO-1, thereby reducing oxidative stress-induced cellular damage [57]. Recent studies have shown that activating the NRF2/HO-1 pathway can alleviate OA progression by modulating the NLRP3 inflammasome [33]. In this study, LOG treatment significantly activated NRF2/HO-1 signaling, reduced ROS production, and alleviated oxidative stress induced by LPS. To further assess this pathway's role, we utilized the NRF2-specific inhibitor ML385, which notably reversed LOG's inhibitory effects on ROS production and NLRP3 inflammasome activation. Interestingly, ML385 abolished the inhibitory effect of LOG on ROS production and NLRP3 inflammasome activation. *In vivo* experiments demonstrated that LOG effectively countered DMM-induced OA, increasing NRF2 expression and reducing NLRP3 expression in articular cartilage.

However, the direct relationship between the ROS-NLRP3-IL-1β axis and the NRF2/HO-1 pathway *in vivo* cannot be solely inferred from the expression levels of these markers. The absence of an NRF2 inhibitor control group in the animal experiments constitutes a significant limitation of this study. Future research should consider including such controls to more definitively parse out the mechanisms by which LOG ameliorates OA, thereby solidifying the therapeutic potential of targeting these pathways in OA treatment strategies.

Conclusion

Our study has demonstrated that LOG can effectively mitigate the progression of OA induced by the destabilization of the DMM. This effect is achieved through the inhibition of ROS-mediated activation of the NLRP3 inflammasome, facilitated by the activation of the NRF2/HO-1 signaling pathway that LOG is able to attenuate DMM-induced OA by inhibiting ROS-mediated activation of NLRP3 inflammasome *via* activating NRF2/HO-1 signaling (Fig. 9). These findings highlight the therapeutic potential of LOG in man-

aging OA, particularly forms associated with inflammation. By targeting key pathways involved in both oxidative stress and inflammatory responses, LOG presents a promising treatment option for inflammatory OA, suggesting its viability for future clinical applications.

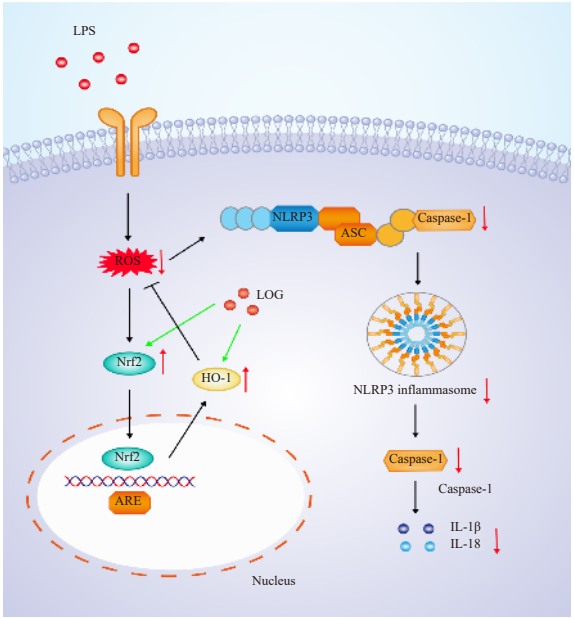

Fig. 9 Potential molecular mechanism of LOG's therapeutic effect in OA.

References

[1] Abramoff B, Caldera FE. Osteoarthritis: pathology, diagnosis, and treatment options [J]. *Med Clin North Am*, 2020, **104**(2): 293-311.

[2] Martel-Pelletier J, Barr AJ, Cicuttini FM, *et al*. Osteoarthritis [J]. *Nat Rev Dis Primers*, 2016, **2**: 16072.

[3] Litwic A, Edwards MH, Dennison EM, *et al*. Epidemiology and burden of osteoarthritis [J]. *Br Med Bull*, 2013, **105**: 185-199.

[4] Di Francesco M, Fragassi A, Pannuzzo M, *et al*. Management of osteoarthritis: from drug molecules to nano/micromedicines [J]. *Wiley Interdiscip Rev Nanomed Nanobiotechnol*, 2022, **14**(3): e1780.

[5] Bindu S, Mazumder S, Bandyopadhyay U. Non-steroidal anti-inflammatory drugs (NSAIDs) and organ damage: a current perspective [J]. *Biochem Pharmacol*, 2020, **180**: 114147.

[6] Palazzo C, Nguyen C, Lefevre-Colau MM, *et al*. Risk factors and burden of osteoarthritis [J]. *Ann Phys Rehabil Med*, 2016, **59**(3): 134-138.

[7] van den Bosch MHJ. Inflammation in osteoarthritis: is it time to dampen the alarm(in) in this debilitating disease [J]. *Clin Exp Immunol*, 2019, **195**(2): 153-166.

[8] McAllister MJ, Chemaly M, Eakin AJ, *et al*. NLRP3 as a potentially novel biomarker for the management of osteoarthritis [J]. *Osteoarthritis Cartilage*, 2018, **26**(5): 612-619.

[9] An S, Hu H, Li Y, *et al*. Pyroptosis plays a role in osteoarthritis [J]. *Aging Dis*, 2020, **11**(5): 1146-1157.

[10] Mangan MSJ, Olhava EJ, Roush WR, *et al*. Targeting the NLRP3 inflammasome in inflammatory diseases [J]. *Nat Rev Drug Discov*, 2018, **17**(8): 588-606.

[11] Ansari MY, Ahmad N, Haqqi TM. Oxidative stress and inflammation in osteoarthritis pathogenesis: role of polyphenols [J]. *Biomed Pharmacother*, 2020, **129**: 110452.

[12] Bolduc JA, Collins JA, Loeser RF. Reactive oxygen species, aging and articular cartilage homeostasis [J]. *Free Radic Biol Med*, 2019, **132**: 73-82.

[13] Minutoli L, Puzzolo D, Rinaldi M, *et al*. ROS-mediated NLRP3 inflammasome activation in brain, heart, kidney, and testis ischemia/reperfusion injury [J]. *Oxid Med Cell Longev*, 2016, **2016**: 2183026.

[14] Liu X, Zhang X, Ding Y, *et al*. Nuclear factor E2-related factor-2 negatively regulates NLRP3 inflammasome activity by inhibiting reactive oxygen species-induced NLRP3 priming [J]. *Antioxid Redox Signal*, 2017, **26**(1): 28-43.

[15] Dai Y, Zhang J, Xiang J, *et al*. Calcitriol inhibits ROS-NLRP3-IL-1β signaling axis *via* activation of Nrf2-antioxidant signaling in hyperosmotic stress stimulated human corneal epithelial cells [J]. *Redox Biol*, 2019, **21**: 101093.

[16] Hamarsheh S, Osswald L, Saller BS, *et al*. Oncogenic Kras(G12D) causes myeloproliferation *via* NLRP3 inflammasome activation [J]. *Nat Commun*, 2020, **11**(1): 1659.

[17] Dodson M, de la Vega MR, Cholanians AB, *et al*. Modulating NRF2 in disease: timing is everything [J]. *Annu Rev Pharmacol Toxicol*, 2019, **59**: 555-575.

[18] Zeng J, Chen Y, Ding R, *et al*. Isoliquiritigenin alleviates early brain injury after experimental intracerebral hemorrhage *via* suppressing ROS- and/or NF-kappaB-mediated NLRP3 inflammasome activation by promoting Nrf2 antioxidant pathway [J]. *J Neuroinflammation*, 2017, **14**(1): 119.

[19] Chen Z, Zhong H, Wei J, *et al*. Inhibition of Nrf2/HO-1 signaling leads to increased activation of the NLRP3 inflammasome in osteoarthritis [J]. *Arthritis Res Ther*, 2019, **21**(1): 300.

[20] Li X, Ye F, Li L, *et al*. The role of HO-1 in protection against lead-induced neurotoxicity [J]. *Neurotoxicology*, 2016, **52**: 1-11.

[21] Huang Y, Li W, Su ZY, *et al*. The complexity of the Nrf2 pathway: beyond the antioxidant response [J]. *J Nutr Biochem*, 2015, **26**(12): 1401-1413.

[22] Loboda A, Damulewicz M, Pyza E, *et al*. Role of Nrf2/HO-1 system in development, oxidative stress response and diseases: an evolutionarily conserved mechanism [J]. *Cell Mol Life Sci*, 2016, **73**(17): 3221-3247.

[23] Wan Y, Shen K, Yu H, *et al*. Baicalein limits osteoarthritis development by inhibiting chondrocyte ferroptosis [J]. *Free Radic Biol Med*, 2023, **196**: 108-120.

[24] Wu J, Li H, Hu F, *et al*. Stevioside attenuates osteoarthritis *via* regulating Nrf2/HO-1/NF-κB pathway [J]. *J Orthop Translat*, 2023, **38**: 190-202.

[25] Chen H, Qin J, Shi H, *et al*. Rhoifolin ameliorates osteoarthritis *via* the Nrf2/NF-κB axis: *in vitro* and *in vivo* experiments [J]. *Osteoarthritis Cartilage*, 2022, **30**(5): 735-745.

[26] Shi Y, Chen J, Li S, *et al*. Tangeretin suppresses osteoarthritis progression *via* the Nrf2/NF-κB and MAPK/NF-κB signaling pathways [J]. *Phytomedicine*, 2022, **98**: 153928.

[27] Hu J, Zhou J, Wu J, *et al*. Loganin ameliorates cartilage degeneration and osteoarthritis development in an osteoarthritis mouse model through inhibition of NF-kappaB activity and pyroptosis in chondrocytes [J]. *J Ethnopharmacol*, 2020, **247**: 112261.

[28] Yang Y, Gu Y, Zhao H, *et al*. Loganin attenuates osteoarthritis in rats by inhibiting IL-1beta-induced catabolism and apoptosis in chondrocytes *via* regulation of phosphatidylinositol 3-kinases (PI3K)/Akt [J]. *Med Sci Monit*, 2019, **25**: 4159-4168.

[29] Huang J, Zhang Y, Dong L, *et al*. Ethnopharmacology, phytochemistry, and pharmacology of *Cornus officinalis* Sieb. et Zucc [J]. *J Ethnopharmacol*, 2018, **213**: 280-301.

[30] Huang F, Wang X, Xiao G, *et al*. Loganin exerts a protective effect on ischemia-reperfusion-induced acute kidney injury by regulating JAK2/STAT3 and Nrf2/HO-1 signaling pathways [J]. *Drug Dev Res*, 2022, **83**(1): 150-157.
[31] Cheng YC, Chu LW, Chen JY, *et al.* Loganin attenuates high glucose-induced schwann cells pyroptosis by inhibiting ROS generation and NLRP3 inflammasome activation [J]. *Cells*, 2020, **9**(9): 1948.
[32] Pan Z, He Q, Zeng J, *et al*. Naringenin protects against iron overload-induced osteoarthritis by suppressing oxidative stress [J]. *Phytomedicine*, 2022, **105**: 154330.
[33] Yan Z, Qi W, Zhan J, *et al*. Activating Nrf2 signalling alleviates osteoarthritis development by inhibiting inflammasome activation [J]. *J Cell Mol Med*, 2020, **24**(22): 13046-13057.
[34] Fang H, Huang L, Welch I, *et al*. Early changes of articular cartilage and subchondral bone in the DMM mouse model of osteoarthritis [J]. *Sci Rep*, 2018, **8**(1): 2855.
[35] Du Q, Fu YX, Shu AM, *et al*. Loganin alleviates macrophage infiltration and activation by inhibiting the MCP-1/CCR2 axis in diabetic nephropathy [J]. *Life Sci*, 2021, **272**: 118808.
[36] Alizadeh SH, Wanlin T, Chen X, *et al*. Cartilage tissue engineering approaches need to assess fibrocartilage when hydrogel constructs are mechanically loaded [J]. *Front Bioeng Biotechnol*, 2022, **9**: 787538.
[37] Henrotin YE, Bruckner P, Pujol JP. The role of reactive oxygen species in homeostasis and degradation of cartilage [J]. *Osteoarthritis Cartilage*, 2003, **11**(10): 747-755.
[38] Kelley N, Jeltema D, Duan Y, *et al.* The NLRP3 inflammasome: an overview of mechanisms of activation and regulation [J]. *Int J Mol Sci*, 2019, **20**(13): 3328.
[39] Zhang DD. Mechanistic studies of the Nrf2-Keap1 signaling pathway [J]. *Drug Metab Rev*, 2006, **38**(4): 769-789.
[40] Baird L, Yamamoto M. The molecular mechanisms regulating the KEAP1-NRF2 pathway [J]. *Mol Cell Biol*, 2020, **40**(13): e00099-20.
[41] Bai Y, Gong X, Dou C, *et al*. Redox control of chondrocyte differentiation and chondrogenesis [J]. *Free Radic Biol Med*, 2019, **132**: 83-89.
[42] El AM, Angulo J, Rodriguez-Manas L. Oxidative stress and vascular inflammation in aging [J]. *Free Radic Biol Med*, 2013, **65**: 380-401.
[43] Portal-Nunez S, Esbrit P, Alcaraz MJ, *et al*. Oxidative stress, autophagy, epigenetic changes and regulation by miRNAs as potential therapeutic targets in osteoarthritis [J]. *Biochem Pharmacol*, 2016, **108**: 1-10.
[44] Biao Y, Chen J, Liu C, *et al*. Protective effect of Danshen Zexie Decoction against non-alcoholic fatty liver disease through inhibition of ROS/NLRP3/IL-1beta pathway by Nrf2 signaling activation [J]. *Front Pharmacol*, 2022, **13**: 877924.
[45] Chu J, Yan B, Zhang J, *et al*. Casticin attenuates osteoarthritis-related cartilage degeneration by inhibiting the ROS-mediated NF-kappaB signaling pathway *in vitro* and *in vivo* [J]. *Inflammation*, 2020, **43**(3): 810-820.
[46] Abais JM, Xia M, Zhang Y, *et al*. Redox regulation of NLRP3 inflammasomes: ROS as trigger or effector [J]. *Antioxid Redox Signal*, 2015, **22**(13): 1111-1129.
[47] Kawai T, Akira S. Toll-like receptors and their crosstalk with other innate receptors in infection and immunity [J]. *Immunity*, 2011, **34**(5): 637-650.
[48] Bording-Jorgensen M, Alipour M, Danesh G, *et al*. Inflammasome activation by ATP enhances citrobacter rodentium clearance through ROS generation [J]. *Cell Physiol Biochem*, 2017, **41**(1): 193-204.
[49] Han Y, Xu X, Tang C, *et al*. Reactive oxygen species promote tubular injury in diabetic nephropathy: the role of the mitochondrial ROS-TXNIP-NLRP3 biological axis [J]. *Redox Biol*, 2018, **16**: 32-46.
[50] Bauernfeind F, Bartok E, Rieger A, *et al*. Cutting edge: reactive oxygen species inhibitors block priming, but not activation, of the NLRP3 inflammasome [J]. *J Immunol*, 2011, **187**(2): 613-617.
[51] Lin C, Ge L, Tang L, *et al*. Nitidine chloride alleviates inflammation and cellular senescence in murine osteoarthritis through scavenging ROS [J]. *Front Pharmacol*, 2022, **13**: 919940.
[52] Vajjhala PR, Mirams RE, Hill JM. Multiple binding sites on the pyrin domain of ASC protein allow self-association and interaction with NLRP3 protein [J]. *J Biol Chem*, 2012, **287**(50): 41732-41743.
[53] He Y, Hara H, Nunez G. Mechanism and regulation of NLRP3 inflammasome activation [J]. *Trends Biochem Sci*, 2016, **41**(12): 1012-1021.
[54] Swanson KV, Deng M, Ting JP. The NLRP3 inflammasome: molecular activation and regulation to therapeutics [J]. *Nat Rev Immunol*, 2019, **19**(8): 477-489.
[55] Li Z, Huang Z, Zhang H, *et al*. P2X7 receptor induces pyroptotic inflammation and cartilage degradation in osteoarthritis *via* NF-kappaB/NLRP3 crosstalk [J]. *Oxid Med Cell Longev*, 2021, **2021**: 8868361.
[56] Ni B, Pei W, Qu Y, *et al*. MCC950, the NLRP3 inhibitor, protects against cartilage degradation in a mouse model of osteoarthritis [J]. *Oxid Med Cell Longev*, 2021, **2021**: 4139048.
[57] Sanada Y, Tan SJO, Adachi N, *et al.* Pharmacological targeting of heme oxygenase-1 in osteoarthritis [J]. *Antioxidants (Basel)*, 2021, **10**(3): 419.

Cite this article as: LI Miao, XIAO Jiacong, CHEN Baihao, *et al*. Loganin inhibits the ROS-NLRP3-IL-1β axis by activating the NRF2/HO-1 pathway against osteoarthritis [J]. *Chin J Nat Med*, 2024, **22**(11): 977-990.